

Decorated Clusters and Geometrical Frustration in Cluster Spin Glass: A Random Graph Approach

S. G. Magalhães^a, F. M. Zimmer^b, R. Erichsen Jr.^a

^a*Instituto de Física, Universidade Federal do Rio Grande do Sul, Porto Alegre, 91501-970, RS, Brazil*

^b*Instituto de Física, Universidade Federal do Mato Grosso do Sul, Campo Grande, MS, Brazil*

Abstract

We develop a theory to investigate how geometrically frustrated clusters that become decorated affect the Cluster Spin Glass phase. The cluster structure is assumed to be a tetrahedron composed of Ising spins with z-anisotropy placed at its vertices that interact antiferromagnetically. We consider the probability $1 - p_J$ of finding an impurity at a vertex of the tetrahedron that interacts ferromagnetically with the remaining elements inside the tetrahedron. An intercluster disorder is added as a random Gaussian interaction. The order parameters are obtained using the sparse random graph technique, which introduces the connectivity of the network of clusters as a controllable parameter in the theory. We examine changes that occur in the Cluster Spin Glass phase as a function of p_J and c , in addition to the antiferromagnetic intracluster couplings J_1 . For intermediate values of p_J , unexpected results appear. Even when some clusters contain a ferromagnetic impurity, there will still be robust geometric frustration effects in the cluster network. However, the p_J threshold for this to occur depends on connectivity. Conversely, below this threshold, reduced GF effects favor the reappearance of the CSG phase. Furthermore, the Curie-Weiss temperature Θ_W has a gradual change of signal, indicating that the effects of the impurities extend to the paramagnetic phase.

Keywords: Disordered systems, Finite connectivity,

PACS: 64.60.De, 87.19.lj, 87.19.lg

Email addresses: `sgmagal@gmail.com` (S. G. Magalhães), `fabiozimmer@gmail.com` (F. M. Zimmer), `rubem@if.ufrgs.br` (R. Erichsen Jr.)

1. Introduction

The frustration effects on spin systems have such complexity that they took the corresponding theory down a fertile path of conceptual innovation [1]. For example, the theory proposed to deal with frustration and quenched disorder has generated such an overpowering conceptual framework [2, 3] that it spilled into other areas of knowledge as distinct as, for example, biology [4] and information theory and combinatorial optimization [5]. Interestingly, the combination of frustration and disorder can also boost new platforms for magnetic materials containing innovative functionalities. One of the most promising possibilities comes from clusters of spins. A possible area of interest for this platform would be, for instance, molecular nanomagnetism [6, 7]. Furthermore, recently, the inclusion of Geometric Frustration (GF) in the description of cluster system having Cluster Spin Glass (CSG) phase, besides its intriguing scientific issues, has acquired technological interest. That is due to its potential to enhance the magnetocaloric effect [8, 9, 10]. However, little consideration has been given to describe how the decorated cluster, defined as those with an inner disorder, interfere with GF, affecting, as a result, the CSG phase.

The high degeneracy introduced by geometrical frustration can make the system extremely sensitive to small perturbations. A common source of perturbation is disorder, which is inevitable due to imperfections in real physical systems. In geometrically frustrated systems, even a very small amount of disorder can have a significant impact, often driving the system into a glassy state. For instance, results reported for the pyrochlore lattice claim that a spin-glass state can be found in the presence of very low levels of quenched disorder [11, 12]. Furthermore, the presence of small frustrated clusters can enhance the effects of disorder, acting as an important mechanism for the freezing process and the stabilization of glassy order in weakly disordered frustrated systems [13, 14].

In spin systems with clusters, the non-trivial ergodicity breaking of the SG can be described within the so-called SG Cluster model [15, 16]. This theory has a random infinite-range intercluster couplings and an intracluster part where the spins are bonded with ferromagnetic (FE) or antiferromagnetic (AF) couplings. The random intercluster part can be handled at the mean-field level using the replica method [17, 18, 19]. As a result, the combination of infinite-ranged random couplings with locally ones, allow the stabilization of a Cluster Spin Glass (CSG) phase. Moreover, the intracluster part of the SG Cluster model requires a solver for each cluster structure. Thus, GF can be introduced by choosing tetrahedral, triangular, or kagome clusters with AF couplings. For frustrated triangular and kagomé clusters, the CSG phase is robust even for infinitesimal random interaction between clusters [20, 21, 22, 23]. These previous works deal with locally ordered clusters. In contrast, here we deal

with clusters that are decorated with a ferromagnetic impurity, introducing local disorder. Would the inner disorder of the cluster suppress the effects of GF? Would be the CSG phase destabilized or reinforced?

To answer properly the above questions, we propose going beyond the mean-field approximation. Indeed, this approximation corresponds to the rather artificial limit of fully connected clusters. Instead, in this work, we adopt an alternative approach using sparse random graphs (SRG) [24, 25, 26], where the connectivity appears as a random variable [27, 28]. As a result, it becomes a controllable parameter within the theory.

Therefore, we aim to investigate how clusters of spins, that were initially geometrically frustrated, affect the stability of the CSG phase when they become decorated. We start assuming a lattice of random interacting clusters of Ising spins as in the SG Cluster model. However, instead of using the mean-field approximation, we use SRG. Thus, the cluster system is transformed into a network of clusters with connectivity following a Poissonian distribution. Moreover, we initially consider clusters with a tetrahedral structure composed of Ising spins with z-anisotropy placed at its vertices that interact antiferromagnetically. Then, a disorder is introduced that allows a given vertex of the tetrahedron to be randomly occupied by an impurity with probability $1 - p_J$ with the spin impurity interacting ferromagnetically with the remaining spins of the tetrahedron.

We use the replica method [25] to deal with the disordered intercluster random interaction. In other words, the SRG replicated partition function is obtained within the replica symmetry solution (RS) [23]. However, since the RS solution is unstable, to mark this instability, the CSG boundary phase line is also obtained by the two-replica method [29].

The paper is organized as follows: the model and theoretical framework are presented in Section 2. Section 3 presents the numerical results and discussions. Conclusions and further remarks are given in Section 4.

2. The Model and Theoretical Framework

We consider a random network composed of N_c interacting clusters, each of them composed of p spins assuming unidirectional Ising spin states with z-axis anisotropy $\sigma_{i\mu} = \pm 1/2$, where $i = 1 \dots p$ is the local index and $\mu = 1 \dots N_c$ is the cluster index. From now on, this random network of interacting clusters will be called the Cluster Network (CN). The clusters interact through their total spin,

$$\sigma_\mu = \sum_{i=1}^p \sigma_{i\mu}. \quad (1)$$

The Hamiltonian is given by

$$H(\boldsymbol{\sigma}, \{J_{\mu\nu}\}, \{J_{ij}\}) = -\frac{1}{\sqrt{c}} \sum_{\mu < \nu, \nu} c_{\mu\nu} J_{\mu\nu} \sigma_\mu \sigma_\nu + \sum_{\mu} H_0(\boldsymbol{\sigma}_\mu, \{J_{ij}\}), \quad (2)$$

where $\boldsymbol{\sigma} = \{\sigma_{i\mu}\}$ represents the state of the whole system, $\boldsymbol{\sigma}_\mu$ represents the state of cluster μ and $J_{\mu\nu}$ are intercluster couplings, randomly chosen from a gaussian distribution with zero average and unitary variance, which is equivalent to fix the energy scale in units of $J_{\mu\nu}$ variance. The elements of the matrix connectivity $c_{\mu\nu}$ are chosen according the binary distribution

$$P(c_{\mu\nu}) = \frac{c}{N_c} \delta_{c_{\mu\nu}, 1} + \left(1 - \frac{c}{N_c}\right) \delta_{c_{\mu\nu}, 0}. \quad (3)$$

The local Hamiltonian H_0 is given by

$$H_0(\boldsymbol{\sigma}_\mu, \{J_{ij}\}) = - \sum_{i < j, j} J_{ij} \sigma_{i\mu} \sigma_{j\mu}, \quad (4)$$

where the J_{ij} are intracuster couplings, to be specified later.

We apply the replica method, assuming that the disorder averaged free energy density (i.e., the free energy per cluster) can be written as

$$f(\beta) = - \lim_{\substack{N_{cl} \rightarrow \infty \\ n \rightarrow 0}} \frac{1}{\beta n N_c} \ln \langle Z^n \rangle, \quad (5)$$

where

$$Z^n = \sum_{\boldsymbol{\sigma}^1 \dots \boldsymbol{\sigma}^n} e^{-\beta \sum_{\alpha=1}^n H(\boldsymbol{\sigma}^\alpha, \{J_{\mu\nu}\}, \{J_{ij}\})} \quad (6)$$

is the replicated partition function, being α the replica index.

Introducing the Hamiltonian, Eq. (2), in the replicated partition function and averaging over the $c_{\mu\nu}$ we obtain, as the leading order in c/N ,

$$\begin{aligned} \langle Z^n \rangle = \sum_{\boldsymbol{\sigma}^1 \dots \boldsymbol{\sigma}^n} \left\langle \exp \left[-\beta \sum_{\alpha\mu} H_0(\boldsymbol{\sigma}_\mu^\alpha, \{J_{ij}\}) + \beta h_e \sum_{\alpha\mu} \sigma_\mu^\alpha \right. \right. \\ \left. \left. + \frac{c}{2N_c} \sum_{\mu \neq \nu} \left\langle e^{\frac{\beta}{\sqrt{c}} J_{\mu\nu} \sum_{\alpha} \sigma_\mu^\alpha \sigma_\nu^\alpha} - 1 \right\rangle_{J_{\mu\nu}} \right] \right\rangle_{\{J_{ij}\}}. \end{aligned} \quad (7)$$

To reduce the problem of a single cluster, the cluster spin variables are withdrawn from the inner exponential by introducing the auxiliary variables $s_\alpha = \sum_{i=1}^p s_i^\alpha$. By

doing so, the partition function becomes

$$\begin{aligned} \langle Z^n \rangle = \sum_{\boldsymbol{\sigma}^1 \dots \boldsymbol{\sigma}^n} \left\langle \exp \left[-\beta \sum_{\alpha\mu} H_0(\boldsymbol{\sigma}_\mu^\alpha, \{J_{ij}\}) + \beta h_e \sum_{\alpha\mu} \sigma_\mu^\alpha \right. \right. \\ \left. \left. + \frac{c}{2N_c} \sum_{\mu \neq \nu} \sum_{\mathbf{s}\mathbf{s}'} \delta_{\mathbf{s}\boldsymbol{\sigma}_\mu} \delta_{\mathbf{s}'\boldsymbol{\sigma}_\nu} \left\langle e^{\frac{\beta J}{\sqrt{c}} \sum_{\alpha} s_{\alpha} s'_{\alpha}} - 1 \right\rangle_J \right] \right\rangle_{J_{\{ij\}}} . \end{aligned} \quad (8)$$

Technical details are left to the Appendix A. The main outcome of the finite connectivity replica calculation is the saddle-point equation

$$W(\mathbf{h}) = \sum_k P_k \int \prod_{l=1}^k d\mathbf{h}_l W(\mathbf{h}_l) \left\langle \prod_{i=1}^4 \delta \left(h_i - \sum_l \phi_i(\mathbf{h}_l, J_l, \{J_{ij}^l\}) \right) \right\rangle_{\{J_l\}, \{J_{ij}^l\}}, \quad (9)$$

where $W(\mathbf{h})$ is the distribution of the p -component local fields \mathbf{h} , the P_k are poissonian weights and the $\phi_i(\mathbf{h}_l, J_l, \{J_{ij}^l\})$ are functions defined in the Appendix A. The method to solve this equation will be explained below.

The RS free-energy density is obtained by introducing the RS *Ansatz* in Eq. (A.4), resulting

$$\begin{aligned} f(\beta) = \frac{c}{2\beta} \int d\mathbf{h} d\mathbf{h}' W(\mathbf{h}) W(\mathbf{h}') \left\langle \ln \frac{\bar{\chi}(\mathbf{h}, \mathbf{h}', J, \{J_{ij}\}, \{J'_{ij}\})}{\chi(0, \mathbf{h}, 0, \{J_{ij}\}) \chi(0, \mathbf{h}', 0, \{J'_{ij}\})} \right\rangle_{J, \{J_{ij}\}, \{J'_{ij}\}} \\ - \frac{1}{\beta} \sum_k P_k \int \prod_l d\mathbf{h}_l W(\mathbf{h}_l) \left\langle \ln \sum_{\mathbf{s}} e^{\beta(-H_0(\mathbf{s}, \{J_{ij}\}) + h_e s)} \right. \\ \left. \times \prod_l \frac{\chi(s, \mathbf{h}_l, J_l, \{J_{ij}\})}{\chi(0, \mathbf{h}_l, 0, \{J_{ij}\})} \right\rangle_{\{J_l\}, \{J_{ij}\}}, \end{aligned} \quad (10)$$

where

$$\begin{aligned} \bar{\chi}(\mathbf{h}, \mathbf{h}', J, \{J_{ij}\}, \{J'_{ij}\}) = \sum_{\mathbf{s}\mathbf{s}'} \exp \left[-\beta H_0(\mathbf{s}, \{J_{ij}\}) \right. \\ \left. + \beta \mathbf{h} \cdot \mathbf{M}(s) - \beta H_0(\mathbf{s}', \{J'_{ij}\}) + \beta \mathbf{h}' \cdot \mathbf{M}(s') + \beta \frac{J}{\sqrt{c}} s s' \right]. \end{aligned} \quad (11)$$

Other relevant observables are the CSG order parameter and the temperature-dependent square of the total spin of each cluster in the CN given, respectively, by

$$q = \int d\mathbf{h} W(\mathbf{h}) \langle s(\mathbf{h}) \rangle^2 \quad (12)$$

and

$$Q = \int d\mathbf{h} W(\mathbf{h}) \langle s^2(\mathbf{h}) \rangle, \quad (13)$$

where

$$\langle s(\mathbf{h}) \rangle = \left\langle \frac{\sum_{\mathbf{s}} s \exp \left[-\beta H_0(\mathbf{s}, \{J_{ij}\}) + \beta \mathbf{h} \cdot \mathbf{M}(s) \right]}{\sum_{\mathbf{s}} \exp \left[-\beta H_0(\mathbf{s}, \{J_{ij}\}) + \beta \mathbf{h} \cdot \mathbf{M}(s) \right]} \right\rangle_{\{J_{ij}\}}, \quad (14)$$

and

$$\langle s^2(\mathbf{h}) \rangle = \left\langle \frac{\sum_{\mathbf{s}} s^2 \exp \left[-\beta H_0(\mathbf{s}, \{J_{ij}\}) + \beta \mathbf{h} \cdot \mathbf{M}(s) \right]}{\sum_{\mathbf{s}} \exp \left[-\beta H_0(\mathbf{s}, \{J_{ij}\}) + \beta \mathbf{h} \cdot \mathbf{M}(s) \right]} \right\rangle_{\{J_{ij}\}}. \quad (15)$$

The freezing temperature T_f coincides with the de Almeida-Thouless (AT) line [30], which signals the stability of the RS solution. In the finite connectivity approach, the AT line can be found using the two-replica method [29]. To do so, we calculate the two-replica joint distribution $W(\mathbf{h}_l, \mathbf{h}'_l)$ through the saddle-point equation

$$W(\mathbf{h}, \mathbf{h}') = \sum_k P_k \int \prod_{l=1}^k d\mathbf{h}_l W(\mathbf{h}_l, \mathbf{h}'_l) \quad (16)$$

$$\times \left\langle \prod_{i=1}^4 \left[\delta \left(h_i - \sum_l \phi_i(\mathbf{h}_l, J_l, \{J_{ij}^l\}) \right) \delta \left(h'_i - \sum_l \phi_i(\mathbf{h}'_l, J_l, \{J_{ij}^l\}) \right) \right] \right\rangle_{\{J_l\}, \{J_{ij}^l\}}.$$

The overlap between the two replicas is given by

$$q' = \int d\mathbf{h} d\mathbf{h}' W(\mathbf{h}, \mathbf{h}') \langle s(\mathbf{h}) \rangle \langle s(\mathbf{h}') \rangle. \quad (17)$$

The RS solution is stable if $q = q'$ and unstable otherwise.

3. Results and Discussion

We start with a cluster with tetrahedral geometry. Then, one has four vertices occupied with elements A that have antiferromagnetic (AF) bonds among them. The disorder inside the cluster is introduced by assuming the probability $1 - p_J$ of having



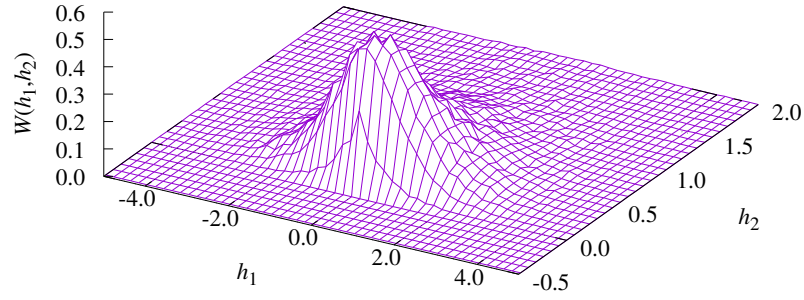
Figure 1: Tetrahedron with solid lines representing ferromagnetic (FE) bonds and dashed lines representing antiferromagnetic (AF) ones. Circles represent the element A and squares represent the impurity B. (a) Ordered, $p_J = 1$ homogeneous tetrahedron with $J_1 = J_{AA} < 0$. (b) Disordered, $p_J = 0$ tetrahedron with $J_1 = J_{AA} < 0$ and $J_1 = J_{AB} > 0$.

one site occupied by an impurity B that has ferromagnetic (FE) bonds with elements A. Thus, the bond disorder inside the cluster is expressed as

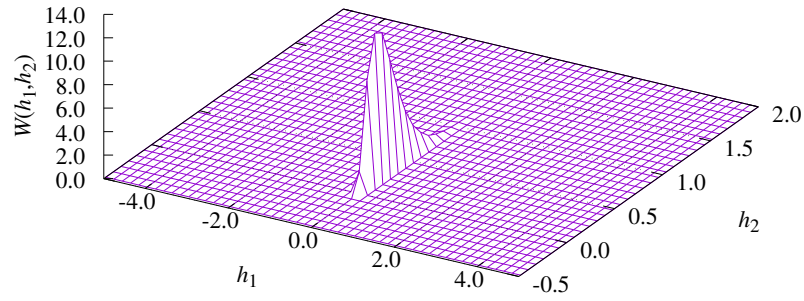
$$P_1(E) = p_J \delta_{E,A} + (1 - p_J) \delta_{E,B}, \quad (18)$$

where $P_1(E)$ is the probability that one vertex of the tetrahedron be occupied by element $E \in \{A, B\}$. The remaining vertices are occupied by element A. To simplify the discussion and avoid increasing the number of parameters, we choose $J_{ij} = J_{AA}$ if the vertices i and j are occupied by the same element A and $J_{ij} = J_{AB}$ if sites i and j are occupied by distinct elements, A and B . The configurations of bonds in the tetrahedron for $p_J = 1$ and 0 are shown in Fig. 1 with $J_{AA} = J_1 = -J_{AB}$. In both scenarios, the tetrahedron is geometrically frustrated. The difference is the total spin of the tetrahedron S_T minimizing the energy and the number of frustrated bonds. Thus, $S_T = 0$ and 1 for $p_J = 1$ and 0, respectively.

We employ a recursive algorithm to solve the fixed-point Eq. (9). A population \mathcal{N} of 4-dimensional vector fields is randomly created. Then for each step, in sequence: (i) an integer k is chosen randomly according to a Poisson distribution; (ii) k 4-components fields are chosen randomly from the population; (iii) the summation appearing in the Dirac's delta function in Eq. (9) is calculated, for each field component and the results are stored in a further field, also randomly chosen from the distribution. This procedure runs till it converges to a stable distribution. The size \mathcal{N} reflects the accuracy of the procedure. The larger the \mathcal{N} , the larger the convergence time t . After some experience we are convinced that the choice $\mathcal{N} = 100,000$ and $t = 20,000,000$, assumed throughout this work, allows to acceptable results. We assume the temperature and J_1 are given in units of J . As an illustration, Fig. 2 reveals the resulting marginal field distributions $W(h_1, h_2)$ for $c = 8$, $p_J = 1$ and $J_1 = -1$. In Fig. 2(a) the temperature is 0.5. A symmetric h_1 distribution represents a CSG phase with a finite order parameter. In Fig. 2(b) the temperature is



(a)



(b)

Figure 2: (a) Marginal distributions $W(h_1, h_2)$ for $c = 8$, $p_J = 1$, $J_1 = -1$ and $T = 0.5$. (b) The same, but for $T = 1.5$.

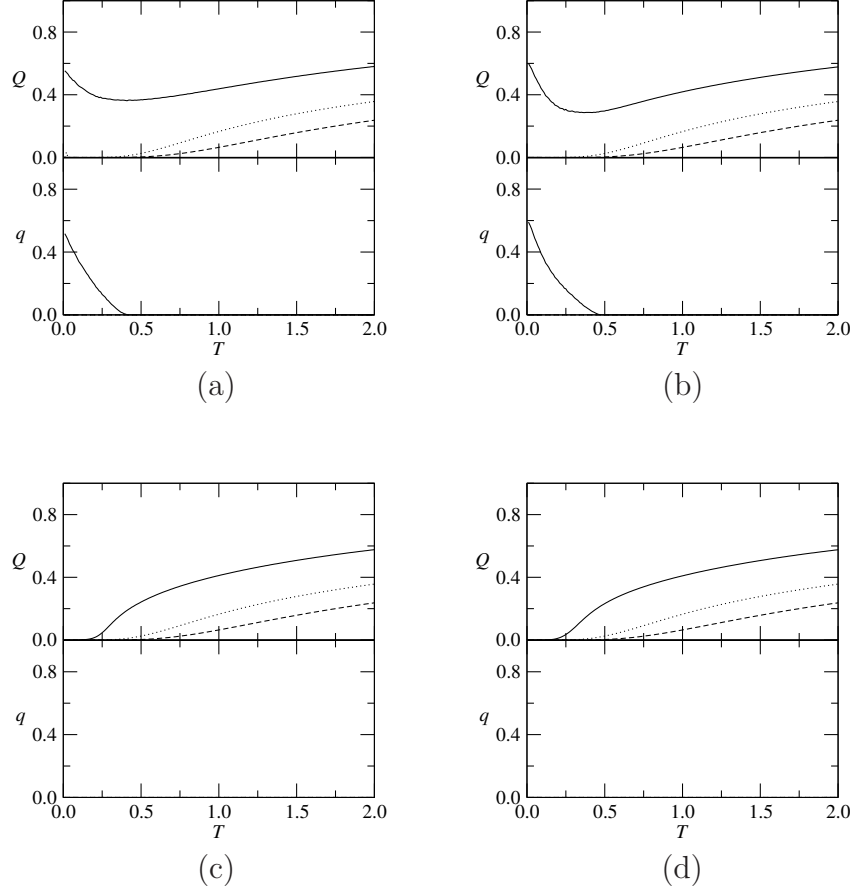


Figure 3: Order parameters Q and q versus temperature T for $p_J = 1$; $J_1 = -2$ (solid), $J_1 = -4$ (dotted) and $J_1 = -6$ (dashed). (a) $c = 2$; (b) $c = 4$; (c) $c = 8$; (d) $c = 12$.

1.5. This time, the marginal $W(h_1)$ is a delta-shaped distribution corresponding to null order parameter, typical of a paramagnetic (PM) phase.

Figs. 3-5 show the behavior of the order parameters q and Q versus the temperature. We start the discussion with the undecorated tetrahedron, $p_J = 1$, where the conditions to the appearing of a CSG phase are met only for low connectivity values, e.g. $c = 2$ and $c = 4$, and weak AF intracluster coupling, e.g. $-J_1 \leq 2$. The order parameter Q shows a non-monotonic behavior, while the order parameter q decreases monotonously to zero at a c -dependent T_f . In the absence of a low-temperature CSG phase for $c = 8$ and $c = 12$, Q is zero at $T = 0$ and then increases monotonically as the temperature increases. The presence of a CSG phase in this condition can be understood by means of the fluctuations induced by the disordered intercluster

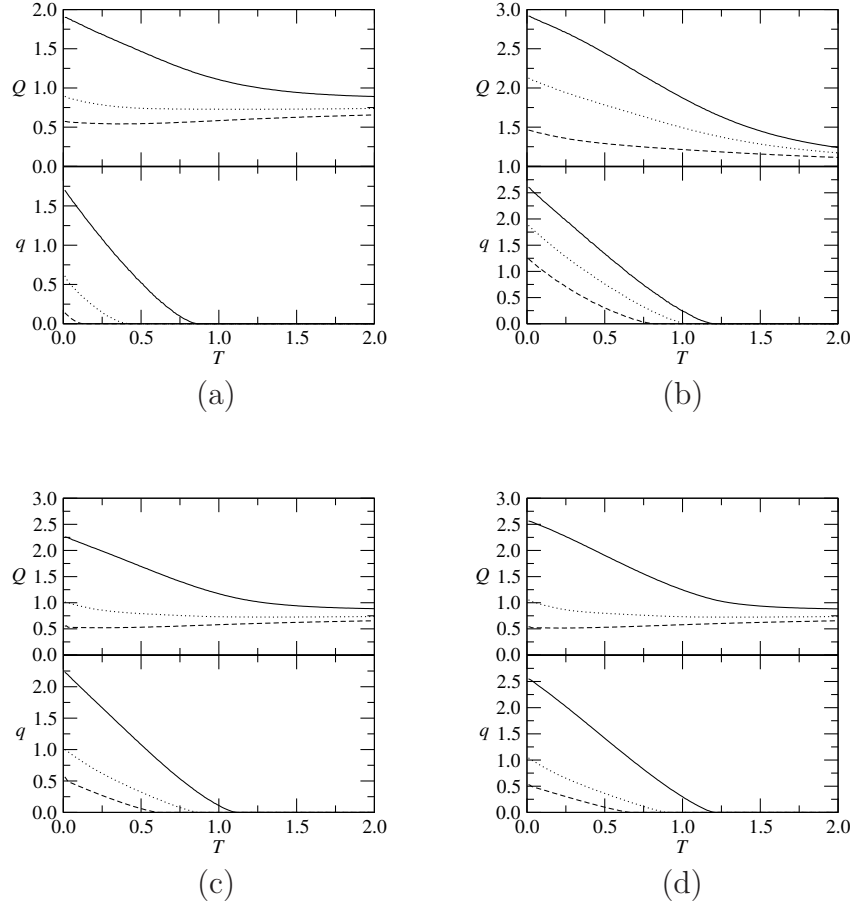


Figure 4: Order parameters Q and q versus temperature T for $p_J = 0.5$; $J_1 = -2$ (solid), $J_1 = -4$ (dotted) and $J_1 = -6$ (dashed). (a) $c = 2$; (b) $c = 4$; (c) $c = 8$; (d) $c = 12$.

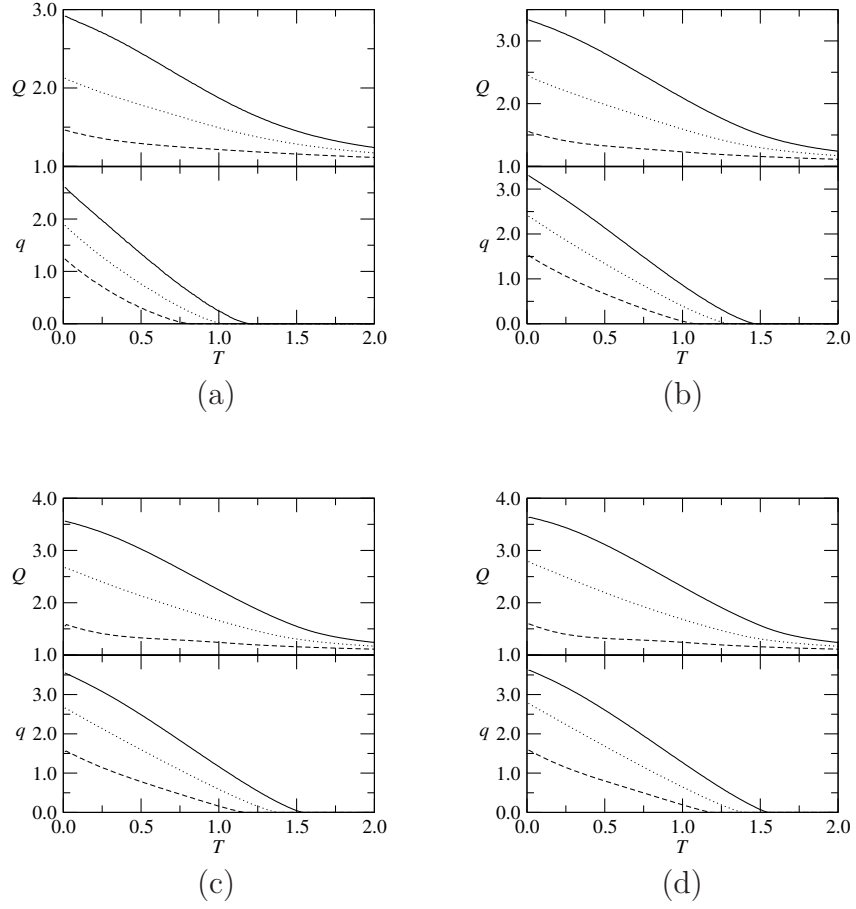


Figure 5: Order parameters Q and q versus temperature T for $p_J = 0$; $J_1 = -2$ (solid), $J_1 = -4$ (dotted) and $J_1 = -6$ (dashed). (a) $c = 2$; (b) $c = 4$; (c) $c = 8$; (d) $c = 12$.

couplings. These fluctuations, being larger for smaller c values, can stabilize a CSG phase for $J_1 = -2$ and $c = 2$ or $c = 4$, but not for larger c or $|J_1|$. The way the fluctuations induces the CSG phase deserves an explanation. Consider $c = 2$. This means that several clusters will have only one neighbor and they will strongly influence each other. In this case, the intercluster coupling may favor tetrahedron states $S_T \neq 0$. Conversely, if c is large, the probability to favor states $S_T \neq 0$ will be smaller, since the cluster neighborhood will be more equally distributed. Furthermore, the long-range couplings are normalized to $1/\sqrt{c}$ (see Eq. 2).

If $0 < p_J < 1$, part of the tetrahedrons in the CN are decorated. In contrast, for $p_J = 0$, the CN is composed with every tetrahedron having a ferromagnetic impurity, called from now on, fully decorated. Now, for both cases, the CSG phase does not result from fluctuations, but from the interactions between the decorated tetrahedrons, which increase with c . This time, contrary to $p_J = 1$, is the large connectivity and the weakening of GF effects in the CN that favor the CSG phase. The case $p_J = 0.5$ is shown in Fig. 4. Except for $c = 2$ and $J_1 = -6$, the freezing temperature T_f is always finite. However, the precise location of T_f depends on c and J_1 values. A similar picture is observed for $p_J = 0$ (see Fig. 5). This time, the presence of the ferromagnetic impurity in every tetrahedron favors larger Q and q states overall and higher T_f values.

To summarize our findings on the order parameters behavior, Fig. 6 displays phase diagrams T vs p_J vs J_1 elaborated from solutions for q and Q in Eqs. (12)-(13). The CN connectivity is ranging from $c = 2$ to $c = 12$. For $p_J = 0$, the freezing temperature T_f is finite for any value of J_1 and c . However, it is worthwhile to remark that T_f decreases for smaller values of c and larger $-J_1$. In contrast, for instance, for $J_1 = -3$, there is suppression of the CSG phase at $p_J^* \approx 0.9$ for any value of c . Moreover, with larger fixed $-J_1$, the role of c is amplified, i.e., a smaller c further decreases the value of p_J^* where the CSG is suppressed. Thus, reinforcing the hypothesis that GF effects in the CN are also strengthened by c besides the intracluster coupling J_1 , leading to a decreasing p_J^* . This possibility is discussed below examining the entropy.

Next, we discuss the entropy density s as a function of the temperature. Fig. 7 shows s versus T for with $p_J = 1$ and several values of CN connectivities and coupling constant J_1 . The independence of the entropy relative to c , except for $J_1 = -2$, demonstrates that the CN itself is governed by the geometrically frustrated undecorated tetrahedrons. So, the CN entropy density converges to a residual entropy density per cluster given as $s_0 = \ln 6$ as $T \rightarrow 0$. Only for $J_1 = -2$, where there is a CSG phase at low temperature, the entropy becomes c -dependent. However, if c is large enough the entropy density also converges to its residual value s_0 , demon-

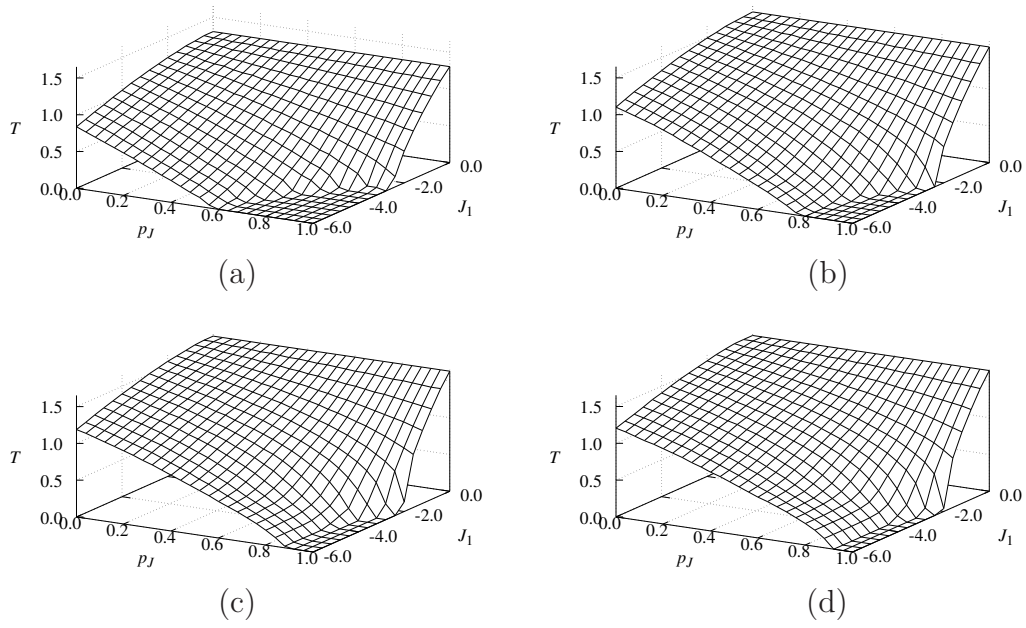
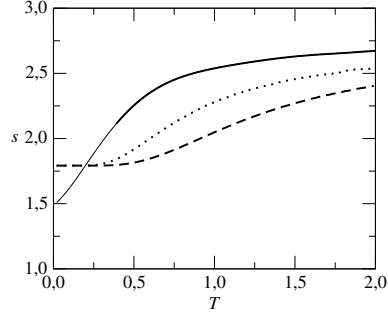
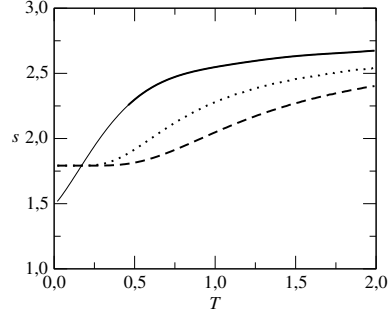


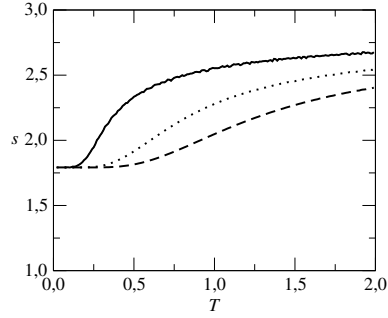
Figure 6: Freezing temperature T_f as a function of p_J and J_1 for some representative connectivity values. (a) $c = 2$; (b) $c = 4$; (c) $c = 8$; (d) $c = 12$.



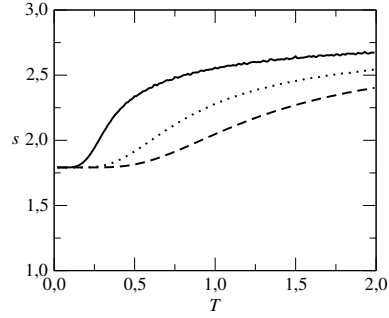
(a)



(b)



(c)



(d)

Figure 7: Entropy density s versus temperature T for $p_J = 1$; $J_1 = -2$ (solid), $J_1 = -4$ (dotted) and $J_1 = -6$ (dashed). (a) $c = 2$; (b) $c = 4$; (c) $c = 6$; (d) $c = 12$. Thick (thin) lines indicates RS stable (unstable) solutions.

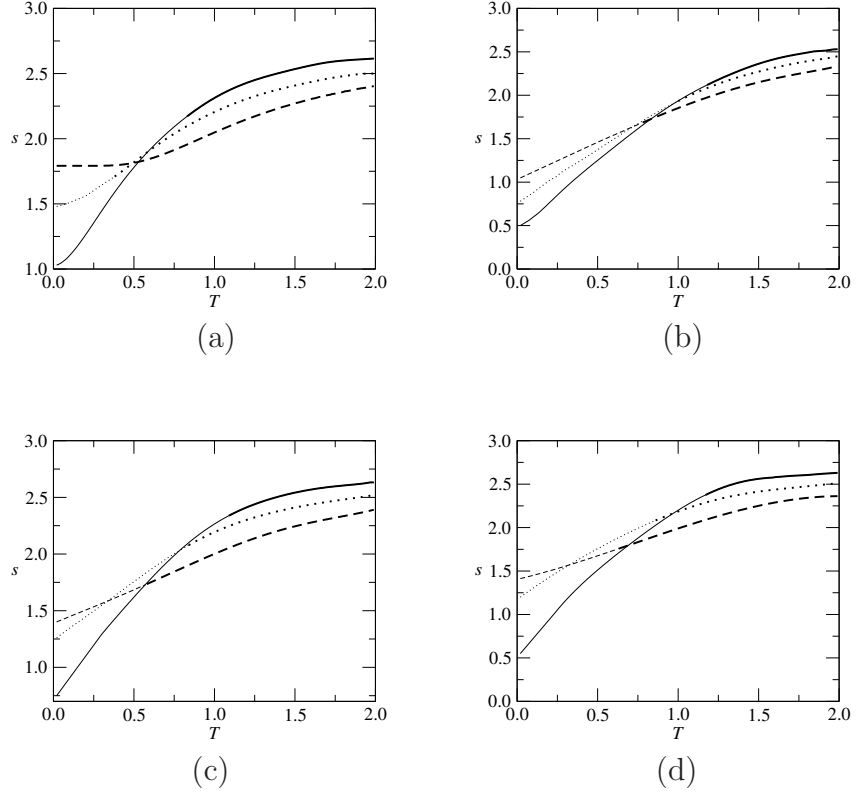


Figure 8: Entropy density s versus temperature T for $p_J = 0.5$; $J_1 = -2$ (solid), $J_1 = -4$ (dotted) and $J_1 = -6$ (dashed). (a) $c = 2$; (b) $c = 4$; (c) $c = 6$; (d) $c = 12$. Thick (thin) lines indicate RS stable (unstable) solutions.

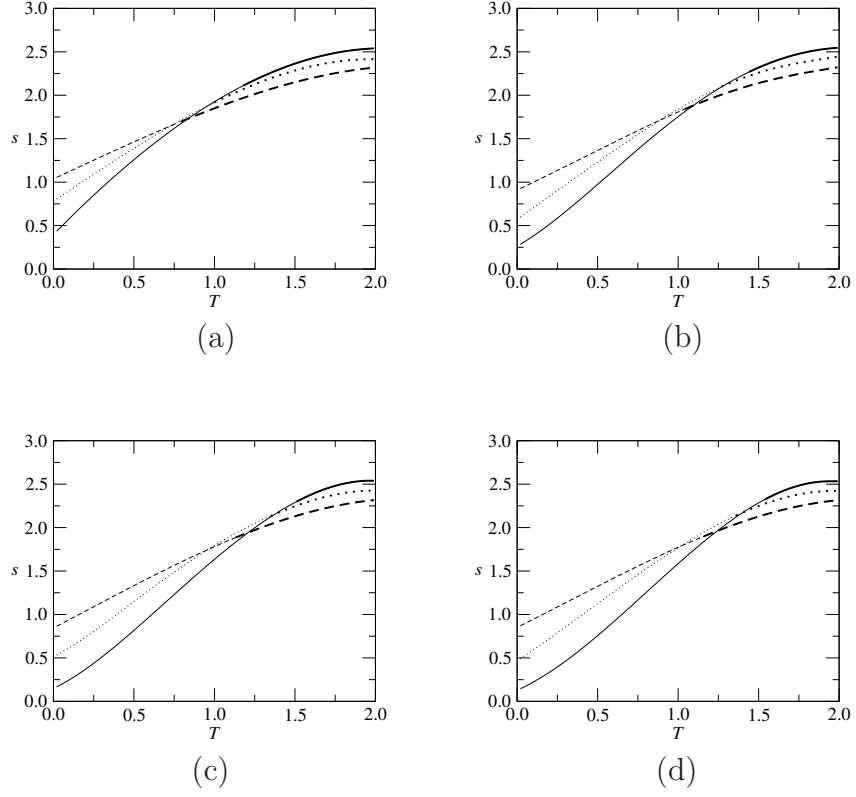


Figure 9: Entropy density s versus temperature T for $p_J = 0$; $J_1 = -2$ (solid), $J_1 = -4$ (dotted) and $J_1 = -6$ (dashed). (a) $c = 2$; (b) $c = 4$; (c) $c = 6$; (d) $c = 12$. Thick (thin) lines indicates RS stable (unstable) solutions.

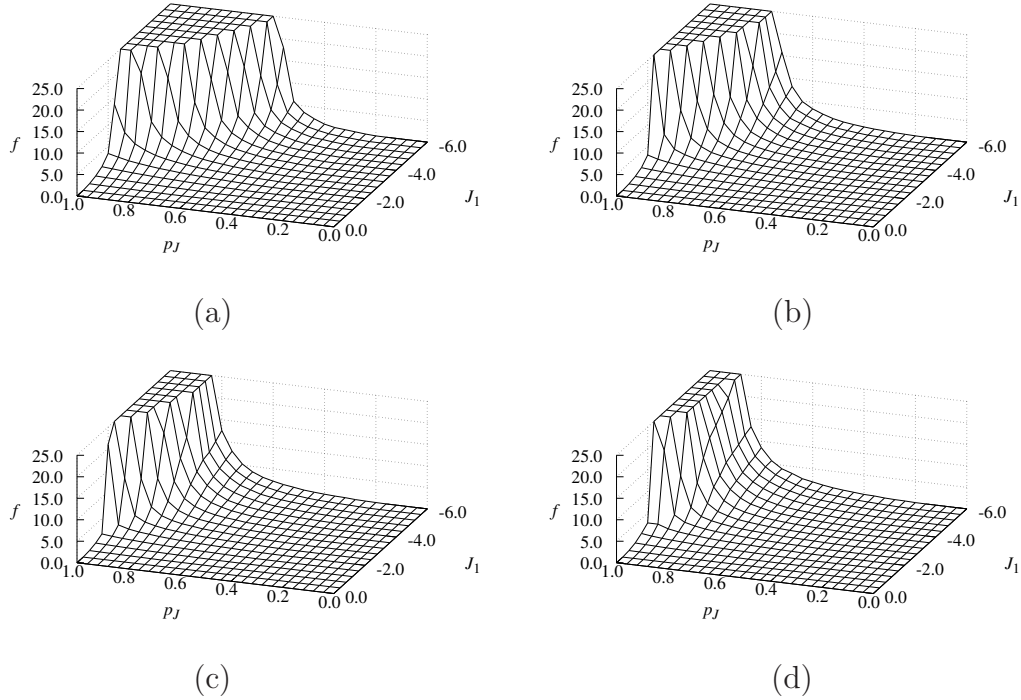


Figure 10: Measure of frustration f vs p_J and J_1 . The connectivity is (a) $c = 2$; (b) $c = 4$; (c) $c = 8$; (d) $c = 12$.

strating that the FG effects become stronger with increasing c associated with the suppression of the CSG phase.

The cases of $p_J = 0.5$ and $p_J = 0$ are shown in Figs. 8 and 9, respectively. For $p_J = 0.5$, only for small c and sufficiently large J_1 (see Fig 8-a) the geometrically frustrated tetrahedrons do prevail in the CN. That leads to the convergence of the entropy density to s_0 and the suppression of the CSG phase, as shown in Fig 4-a. In other words, in contrast to the undecorated case, for $p_J = 0.5$, the GF effects become weaker with increasing c . For the fully decorated case, there is no trace of FG effects. On the contrary, the CSG phase is stabilized in any case shown in Fig. 9. However, the behavior of the entropy density at $T < T_f$ is unreliable due to the instability of the RS solution. The RSB range, marked using the two replica method, is indicated by thin lines in the entropy density curves.

In Fig. 10, a measure of frustration, given by $f_p = -\Theta_W/T_f$ [31, 32] where Θ_W is the Curie-Weiss temperature is shown as a function of p_J and J_1 . The Curie-Weiss temperature is obtained using the usual procedure of extrapolating the high-

temperature behavior of the inverse of susceptibility χ^{-1} to $T = 0$. In Fig. 10, there are parts of the plane p_J versus J_1 where f_p diverges or is null. In the first case (cutoff at $f = 25$), T_f goes to zero, i.e., the CSG phase is suppressed (see Fig. 6) by GF effects. In the second, it is assumed that $f_p = 0$ for $\Theta_W > 0$. Fig. 10 shows that for J_1 sufficiently large, the divergence of f_p occurs even when the CN is partially decorated. However, except for the undecorated case, the region where f_p diverges shrinks as c increases. Interestingly, there is also a gradual change in the sign of Θ_W as the CN changes from fully to partially decorated independently of the connectivity.

4. Concluding remarks

In this work, we developed a theory to describe a network of geometrically frustrated clusters when a portion or even all of them have a defect. We call these decorated clusters. In our theory, defect means specifically the following two steps. Firstly, we assume a tetrahedral cluster structure where all vertices are occupied by elements interacting antiferromagnetically. Then, a ferromagnetic impurity is included with a probability $1 - p_J$ of occupying some vertex in the tetrahedron. Moreover, we use Sparse Random Graph (SGR) technique which allows a description beyond the mean-field approximation. In other words, the connectivity among the clusters is a controllable parameter. In this case, we are dealing with a cluster network. There is also a random interaction between clusters that helps to stabilize a Cluster Spin Glass (CSG) phase. Thus, we draw our conclusions from changes that occur in the CSG phase.

In the undecorate case $p_J = 1$, e.g. none cluster has a ferromagnetic impurity, the GF suppresses the CSG phase except for low connectivity and small antiferromagnetic couplings. In this limit, a mechanism related to the connectivity fluctuations intervenes to stabilize the CSG phase. In the opposite limit $p_J = 0$, the CSG is always stabilized. There is no trace of GF impact on the CSG phase. However, there are some unexpected consequences for $0 < p_J < 1$. For example, even when part of the clusters has a ferromagnetic impurity, there will still be robust GF effects in the cluster network. This is the case as long as the antiferromagnetic couplings within the cluster are sufficiently strong. Nonetheless, the threshold of p_J for this to happen depends on c . Conversely, below this threshold, reduced GF effects favor the reappearance of the CSG phase. Indeed, the presence of ferromagnetic impurities provides a way to replace geometrically frustrated clusters with those in which frustration arises from competition between FE and AF intracluster interactions. These competing interactions produce the same degree of intracluster degeneracy

as the fully geometrically frustrated case. However, the degenerate local (cluster) spin states differ between the two situations: geometrically frustrated clusters produce zero magnetic moments, while FE-AF competition can result in nonzero cluster magnetic moments. The intracluster disorder given by p_J would interpolate between the two situations. We also find a gradual change in the sign of the Curie-Weiss temperature Θ_W as more clusters have ferromagnetic impurities, indicating that the accumulation of defects in the cluster network also manifests itself in the paramagnetic phase.

Lastly, we highlight that the theory presented in this work can be applied to clusters with other geometries. We are currently investigating this problem with cluster structures such as kagomé and triangular [33] as well as using other types of disorder within the cluster. Another direction of investigation in which our type of approach may be useful is artificial spin glass systems consisting of Ising-spin nanomagnets arranged in a Hopfield-type network that have recently been observed [34].

Appendix A. Derivation of the saddle-point equation

We continue with Eq. (8) and introduce the order function

$$P(\mathbf{s}) = \frac{1}{N_c} \sum_{\mu} \delta_{\mathbf{s}\sigma_{\mu}} \quad (\text{A.1})$$

as the probability to find a replica state vector \mathbf{s} and its conjugated order function $\hat{P}(\mathbf{s})$ to obtain

$$\begin{aligned} \langle Z^n \rangle = & \sum_{\sigma^1 \dots \sigma^n} \left\langle \int \prod_{\mathbf{s}} dP(\mathbf{s}) d\hat{P}(\mathbf{s}) \exp \left\{ -\beta \sum_{\alpha\mu} H_0(\sigma_{\mu}^{\alpha}, \{J_{ij}\}) \right. \right. \\ & + \beta h_e \sum_{\alpha\mu} \sigma_{\mu}^{\alpha} + \sum_{\mathbf{s}} \hat{P}(\mathbf{s}) P(\mathbf{s}) - \frac{1}{N_c} \sum_{\mathbf{s}} \hat{P}(\mathbf{s}) \sum_{\mu} \delta_{\mathbf{s}\sigma_{\mu}} \\ & \left. \left. + \frac{cN_c}{2} \sum_{\mathbf{s}\mathbf{s}'} P(\mathbf{s}) P(\mathbf{s}') \left\langle e^{\frac{\beta J}{\sqrt{c}} \sum_{\alpha} s_{\alpha} s'_{\alpha}} - 1 \right\rangle_J \right\} \right\rangle_{\{J_{ij}\}}. \end{aligned} \quad (\text{A.2})$$

Summing over the cluster variables and changing $\hat{P}(\mathbf{s})$ to $N_c \hat{P}(\mathbf{s})$, the partition function becomes

$$\begin{aligned} \langle Z^n \rangle = & \int \prod_{\mathbf{s}} dP(\mathbf{s}) d\hat{P}(\mathbf{s}) \exp N_c \left\{ \sum_{\mathbf{s}} \hat{P}(\mathbf{s}) P(\mathbf{s}) \right. \\ & + \ln \sum_{\mathbf{s}} \left\langle \exp \left[-\beta \sum_{\alpha} H_0(\mathbf{s}^{\alpha}, \{J_{ij}\}) + \beta h_e \sum_{\alpha} s_{\alpha} - \hat{P}(\mathbf{s}) \right] \right\rangle_{\{J_{ij}\}} \\ & \left. + \frac{c}{2} \sum_{\mathbf{s}\mathbf{s}'} P(\mathbf{s}) P(\mathbf{s}') \left\langle e^{\frac{\beta J}{\sqrt{c}} \sum_{\alpha} s_{\alpha} s'_{\alpha}} - 1 \right\rangle_J \right\}. \end{aligned} \quad (\text{A.3})$$

In the limit $N_c \rightarrow \infty$, this integral can be evaluated by the saddle-point method. Eliminating the $\hat{P}(\mathbf{s})$ through the saddle-point equations, we can write the free energy (Eq. 5) as

$$\begin{aligned} f(\beta) = & -\lim_{n \rightarrow 0} \frac{1}{\beta n} \text{Extr} \left\{ -\frac{c}{2} \sum_{\mathbf{s}\mathbf{s}'} P(\mathbf{s}) P(\mathbf{s}') \left\langle e^{\frac{\beta J}{\sqrt{c}} \sum_{\alpha} s_{\alpha} s'_{\alpha}} - 1 \right\rangle_J \right. \\ & + \ln \sum_{\mathbf{s}} \left\langle \exp \left[-\beta \sum_{\alpha} H_0(\mathbf{s}^{\alpha}, \{J_{ij}\}) + \beta h_e \sum_{\alpha} s_{\alpha} \right. \right. \\ & \left. \left. + c \sum_{\mathbf{s}'} P(\mathbf{s}') \left\langle e^{\frac{\beta J}{\sqrt{c}} \sum_{\alpha} s_{\alpha} s'_{\alpha}} - 1 \right\rangle_J \right] \right\rangle_{\{J_{ij}\}} \right\}, \end{aligned} \quad (\text{A.4})$$

where $\text{Extr}\{\cdot\}$ means the extremum relative to $P(\mathbf{s})$. Applying this condition we obtain a self consistent equation for $P(\mathbf{s})$:

$$\begin{aligned} P(\mathbf{s}) = & \frac{1}{\mathcal{N}} \left\langle \exp \beta \sum_{\alpha} \left[-H_0(\mathbf{s}^{\alpha}, \{J_{ij}\}) + h_e s_{\alpha} \right] \right\rangle_{\{J_{ij}\}} \\ & \times \exp \left[c \sum_{\mathbf{s}'} P(\mathbf{s}') \left\langle e^{\frac{\beta J}{\sqrt{c}} \sum_{\alpha} s_{\alpha} s'_{\alpha}} - 1 \right\rangle_J \right], \end{aligned} \quad (\text{A.5})$$

with $\mathcal{N} \equiv \sum_{\mathbf{s}} P(\mathbf{s})$ is a normalization factor. We focus on the replica symmetric (RS) solution of Eq. (A.5), by which the order function remains unchanged under replica permutation. This is expressed by the RS *Ansatz*

$$P(\mathbf{s}) = \int d\mathbf{h} W(\mathbf{h}) \left\langle \frac{\exp \beta \sum_{\alpha} \left[-H_0(\mathbf{s}^{\alpha}, \{J_{ij}\}) + h_e s_{\alpha} + \mathbf{h} \cdot \mathbf{M}(s_{\alpha}) \right]}{\left\{ \sum_{\mathbf{s}} \exp \beta \left[-H_0(\mathbf{s}, \{J_{ij}\}) + h_e s + \mathbf{h} \cdot \mathbf{M}(s) \right] \right\}^n} \right\rangle_{\{J_{ij}\}}, \quad (\text{A.6})$$

where \mathbf{h} and $\mathbf{M}(s) \equiv (s, s^2, \dots, s^p)$ are p components vectors and $W(\mathbf{h})$ is a p component distribution of local fields. Introducing the *Ansatz* in Eq. (A.5) and expanding

the exponential, summing over the spin variables and rearranging terms we have, unless for the normalization factor \mathcal{N} ,

$$P(\mathbf{s}) = \left\langle \exp \beta \sum_{\alpha} [-H_0(\mathbf{s}^{\alpha}, \{J_{ij}\}) + h_e s_{\alpha}] \right\rangle_{\{J_{ij}\}} \quad (\text{A.7})$$

$$\times \sum_k P_k \prod_{l=1}^k \int d\mathbf{h}_l W(\mathbf{h}_l) \left\langle \frac{\exp \sum_{\alpha} \sum_s \delta_{ss_{\alpha}} \ln \chi(s, \mathbf{h}_l, J_l, \{J_{ij}^l\})}{\chi^n(0, \mathbf{h}_l, 0, \{J_{ij}^l\})} \right\rangle_{J_l, \{J_{ij}^l\}},$$

where $p_k = e^{-c} c^k / k!$ is a poissonian weight and

$$\chi(s, \mathbf{h}, J, \{J_{ij}\}) = \sum_{\mathbf{s}'} \exp \beta \left[-H_0(\mathbf{s}', \{J_{ij}\}) + h_e s' + \mathbf{h} \cdot \mathbf{M}(\mathbf{s}') + \frac{J}{\sqrt{c}} s s' \right]. \quad (\text{A.8})$$

The total spin of the tetrahedral, 4-spin cluster can assume five states: -2, -1, 0, 1 and 2 (Eq. 1). The five-state Kröneckers delta reads

$$\delta_{ss_{\alpha}} = 1 - \frac{5}{4}(s^2 + s_{\alpha}^2) + \frac{65}{72} s s_{\alpha} + \frac{1}{4}(s^4 + s_{\alpha}^4) - \frac{17}{72}(s^3 s_{\alpha} + s s_{\alpha}^3) \\ + \frac{707}{288} s^2 s_{\alpha}^2 - \frac{155}{288}(s^4 s_{\alpha}^2 + s^2 s_{\alpha}^4) + \frac{5}{72} s^3 s_{\alpha}^3 + \frac{35}{288} s^4 s_{\alpha}^4. \quad (\text{A.9})$$

Introducing Eq. (A.9) in Eq. (A.7) and summing over s results

$$P(\mathbf{s}) = \left\langle \exp \beta \sum_{\alpha} [-H_0(\mathbf{s}^{\alpha}, \{J_{ij}\}) + h_e s_{\alpha}] \right\rangle_{\{J_{ij}\}} \quad (\text{A.10})$$

$$\times \sum_k P_k \int \prod_{l=1}^k d\mathbf{h}_l W(\mathbf{h}_l) \left\langle \exp \left[\beta \sum_l \phi(\mathbf{h}_l, J_l, \{J_{ij}^l\}) \cdot \sum_{\alpha} \mathbf{M}(s_{\alpha}) \right] \right\rangle_{\{J_l, \{J_{ij}^l\}\}},$$

where $\phi(\mathbf{h}_l, J_l, \{J_{ij}^l\})$ is a vector with components

$$\phi_1(\mathbf{h}, J, \{J_{ij}\}) = \frac{1}{\beta} \left[-\frac{1}{12} \ln \frac{\chi(2, \mathbf{h}, J, \{J_{ij}\})}{\chi(-2, \mathbf{h}, J, \{J_{ij}\})} + \frac{2}{3} \ln \frac{\chi(1, \mathbf{h}, J, \{J_{ij}\})}{\chi(-1, \mathbf{h}, J, \{J_{ij}\})} \right], \quad (\text{A.11})$$

$$\phi_2(\mathbf{h}, J, \{J_{ij}\}) = \frac{1}{\beta} \left[-\frac{1}{24} \ln \chi(2, \mathbf{h}, J, \{J_{ij}\}) \chi(-2, \mathbf{h}, J, \{J_{ij}\}) \right. \\ \left. + \frac{2}{3} \ln \chi(1, \mathbf{h}, J, \{J_{ij}\}) \chi(-1, \mathbf{h}, J, \{J_{ij}\}) - \frac{5}{4} \ln \chi(0, \mathbf{h}, J, \{J_{ij}\}) \right], \quad (\text{A.12})$$

$$\phi_3(\mathbf{h}, J, \{J_{ij}\}) = \frac{1}{\beta} \left[\frac{1}{12} \ln \frac{\chi(2, \mathbf{h}, J, \{J_{ij}\})}{\chi(-2, \mathbf{h}, J, \{J_{ij}\})} - \frac{1}{6} \ln \frac{\chi(1, \mathbf{h}, J, \{J_{ij}\})}{\chi(-1, \mathbf{h}, J, \{J_{ij}\})} \right] \quad (\text{A.13})$$

and

$$\begin{aligned} \phi_4(\mathbf{h}, J, \{J_{ij}\}) = & \frac{1}{\beta} \left[\frac{1}{24} \ln \chi(2, \mathbf{h}, J, \{J_{ij}\}) \chi(-2, \mathbf{h}, J, \{J_{ij}\}) \right. \\ & \left. - \frac{1}{6} \ln \chi(1, \mathbf{h}, J, \{J_{ij}\}) \chi(-1, \mathbf{h}, J, \{J_{ij}\}) + \frac{1}{4} \ln \chi(0, \mathbf{h}, J, \{J_{ij}\}) \right]. \end{aligned} \quad (\text{A.14})$$

Comparing Eq. (A.10) with the RS Ansatz, Eq. (A.6), in the limit $n \rightarrow 0$ we have

$$\begin{aligned} & \int d\mathbf{h} W(\mathbf{h}) \left\langle \exp \beta \sum_{\alpha} \left[-H_0(\mathbf{s}^{\alpha}, \{J_{ij}\}) + h_e s_{\alpha} + \mathbf{h} \cdot \mathbf{M}(s_{\alpha}) \right] \right\rangle_{\{J_{ij}\}} \\ &= \left\langle \exp \beta \sum_{\alpha} \left[-H_0(\mathbf{s}^{\alpha}, \{J_{ij}\}) + h_e s_{\alpha} \right] \right\rangle_{\{J_{ij}\}} \\ & \times \sum_k P_k \int \prod_{l=1}^k d\mathbf{h}_l W(\mathbf{h}_l) \left\langle \exp \left[\beta \sum_l \phi(\mathbf{h}_l, J_l, \{J_{ij}^l\}) \cdot \sum_{\alpha} \mathbf{M}(s_{\alpha}) \right] \right\rangle_{\{J_l\}, \{J_{ij}^l\}}. \end{aligned} \quad (\text{A.15})$$

Introducing a Dirac's δ -function for each field component in the RHS results

$$\begin{aligned} & \int d\mathbf{h} W(\mathbf{h}) \left\langle \exp \beta \sum_{\alpha} \left[-H_0(\mathbf{s}^{\alpha}, \{J_{ij}\}) + h_e s_{\alpha} + \mathbf{h} \cdot \mathbf{M}(s_{\alpha}) \right] \right\rangle_{\{J_{ij}\}} \\ &= \left\langle \exp \beta \sum_{\alpha} \left[-H_0(\mathbf{s}^{\alpha}, \{J_{ij}\}) + h_e s_{\alpha} \right] \right\rangle_{\{J_{ij}\}} \int d\mathbf{h} \sum_k P_k \int \prod_{l=1}^k d\mathbf{h}_l W(\mathbf{h}_l) \\ & \times \left\langle \prod_{i=1}^4 \delta \left(h_i - \sum_l \phi_i(\mathbf{h}_l, J_l, \{J_{ij}^l\}) \right) \exp \left[\beta \mathbf{h} \cdot \sum_{\alpha} \mathbf{M}(s_{\alpha}) \right] \right\rangle_{\{J_l\}, \{J_{ij}^l\}}. \end{aligned} \quad (\text{A.16})$$

Comparing both sides, we obtain the saddle-point equation for the RS distribution of local fields, Eq. (9).

References

- [1] C. Lacroix, P. Mendels, F. Mila, Introduction to Frustrated Magnetism: Materials, Experiments, Theory, Springer, 2011. doi:10.1007/978-3-642-10589-0.
- [2] K. H. Fischer, J. A. Hertz, Spin Glasses, Cambridge Studies in Magnetism, Cambridge University Press, 1991.

- [3] M. Mezard, G. Parisi, M. Virasoro, Spin Glass Theory and Beyond, Lecture Notes in Physics Series, World Scientific, 1987.
URL <https://books.google.com.br/books?id=ZIF9QgAACAAJ>
- [4] A. Pagnani, F. Tria, M. Weigt, Classification and sparse-signature extraction from gene-expression
Journal of Statistical Mechanics: Theory and Experiment 2009 (05) (2009) P05001. doi:10.1088/1742-5468/2009/05/p05001.
URL <https://doi.org/10.1088/1742-5468/2009/05/p05001>
- [5] A. Montanari, N. Sourlas, The statistical mechanics of turbo codes, European Physical Journal B 18 (1) (2000) 107–119. doi:10.1007/PL00011086.
- [6] J. Schnack, Effects of frustration on magnetic molecules: a survey from olivier kahn until today,
Dalton Transactions 39 (20) (2010) 4677–4686. doi:10.1039/b925358k.
URL <https://doi.org/10.1039/b925358k>
- [7] A. Furrer, O. Waldmann, Magnetic cluster excitations, Rev. Mod. Phys. 85 (2013) 367–420. doi:10.1103/RevModPhys.85.367.
URL <https://link.aps.org/doi/10.1103/RevModPhys.85.367>
- [8] F. M. Zimmer, R. Mourao, M. Schmidt, M. A. Tumelero, S. G. Magalhaes, Enhancement of the magnetocaloric effect in geometrically frustrated cluster spin glass systems,
J. Phys.: Cond. Matter 35 (0) (2023) 315801. doi:10.1088/1361-648X/acd040.
URL <https://doi.org/10.1088/1361-648X/acd040>
- [9] J. Kumar, K. Mukherjee, Enhanced cryogenic magnetocaloric performance and the existence of sh
J. Phys. D: Appl. Phys. 57 (2024) 295304. doi:10.1088/1361-6463/ad3bc2.
URL <https://doi.org/10.1088/1361-6463/ad3bc2>
- [10] P. K. Mishra, A. Gautam, H. Singh, S. Panda, N. Mohapatra, A. K. Ganguli, Interplay of Competing Magnetic Interactions in Noncentrosymmetric Nd₃Te₄ for Enhancing the
Chem. Matter 36 (2024) 5986. doi:10.1021/acs.chemmater.4c00453.
URL <https://doi.org/10.1021/acs.chemmater.4c00453>
- [11] Saunders, T. E. and Chalker, J. T., Spin Freezing in Geometrically Frustrated Antiferromagnets with Weak Disorder, Phys. Rev. Lett. 98 (2007) 157201. doi:10.1103/PhysRevLett.98.157201.
- [12] A. Sen, R. Moessner, Topological spin glass in diluted spin ice, Phys. Rev. Lett. 114 (2015) 247207. doi:10.1103/PhysRevLett.114.247207.
URL <https://link.aps.org/doi/10.1103/PhysRevLett.114.247207>

- [13] F. M. Zimmer, W. C. Silva, M. Schmidt, S. G. Magalhaes, Role of frustration in a weakly disordered checkerboard lattice, *Journal of Magnetism and Magnetic Materials* 554 (2022) 169273. doi:10.1016/j.jmmm.2022.169273.
- [14] M. Schmidt, F. Zimmer, S. Magalhaes, Spin glass induced by infinitesimal disorder in geometrically frustrated kagome lattice, *Physica A: Statistical Mechanics and its Applications* 438 (2015) 416–423. doi:10.1016/j.physa.2015.07.010.
- [15] C. M. Soukoulis, K. Levin, Cluster mean-field theory of spin-glasses, *Phys. Rev. Lett.* 39 (1977) 581–584. doi:10.1103/PhysRevLett.39.581.
URL <https://link.aps.org/doi/10.1103/PhysRevLett.39.581>
- [16] C. M. Soukoulis, Thermodynamic properties of concentrated spin glasses: A cluster mean-field theory, *Phys. Rev. B* 18 (1978) 3757–3759. doi:10.1103/PhysRevB.18.3757.
URL <https://link.aps.org/doi/10.1103/PhysRevB.18.3757>
- [17] D. Sherrington, S. Kirkpatrick, Solvable model of a spin-glass, *Phys. Rev. Lett.* 35 (1975) 1792–1796. doi:10.1103/PhysRevLett.35.1792.
URL <https://link.aps.org/doi/10.1103/PhysRevLett.35.1792>
- [18] G. Parisi, A sequence of approximated solutions to the s-k model for spin glasses, *Journal of Physics A: Mathematical and General* 13 (4) (1980) L115–L121. doi:10.1088/0305-4470/13/4/009.
URL <https://doi.org/10.1088/0305-4470/13/4/009>
- [19] G. Parisi, Magnetic properties of spin glasses in a new mean field theory, *Journal of Physics A: Mathematical and General* 13 (5) (1980) 1887–1895. doi:10.1088/0305-4470/13/5/047.
URL <https://doi.org/10.1088/0305-4470/13/5/047>
- [20] F. M. Zimmer, C. F. Silva, S. G. Magalhaes, C. Lacroix, Interplay between spin-glass clusters and geometrical frustration, *Phys. Rev. E* 89 (2014) 022120. doi:10.1103/PhysRevE.89.022120.
URL <https://link.aps.org/doi/10.1103/PhysRevE.89.022120>
- [21] M. Schmidt, F. M. Zimmer, S. G. Magalhaes, Weak randomness in geometrically frustrated systems: spin-glasses, *Physica Scripta* 90 (2) (2015) 025809. doi:10.1088/0031-8949/90/2/025809.
URL <https://doi.org/10.1088/0031-8949/90/2/025809>

- [22] M. Schmidt, F. M. Zimmer, S. G. Magalhaes, Spin liquid and infinitesimal-disorder-driven cluster spin glass in the kagome lattice, *J. Phys.: Condens. Matter* 29 (16) (2017) 165801. doi:10.1088/1361-648x/aa6060. URL <https://doi.org/10.1088/1361-648x/aa6060>
- [23] A. Silveira, R. Erichsen, S. G. Magalhaes, Geometrical frustration and cluster spin glass with random graphs, *Phys. Rev. E* 103 (2021) 051104. doi:10.1103/PhysRevE.103.052110. URL <https://link.aps.org/doi/10.1103/PhysRevE.103.052110>
- [24] M. Mézard, G. Parisi, Mean-Field Theory of Randomly Frustrated Systems with Finite Connectivity, *Europhys. Lett.* 3 (10) (1987) 1067–1074. URL <http://iopscience.iop.org/0295-5075/3/10/002>
- [25] R. Monasson, Optimization problems and replica symmetry breaking in finite connectivity spin glasses, *Journal of Physics A: Mathematical and General* 31 (2) (1998) 513–529. doi:10.1088/0305-4470/31/2/012. URL <https://doi.org/10.1088/0305-4470/31/2/012>
- [26] A. Montanari, Finding One Community in a Sparse Graph, *J Stat Phys* 161 (2015) 273–299. doi:10.1007/s10955-015-1338-2.
- [27] F. L. Metz and I. Pérez Castillo, Condensation of degrees emerging through a first-order phase transition in classical random graphs, *Phys. Rev. E* 100 (2019) 012305. doi:10.1103/PhysRevE.100.012305.
- [28] R. Erichsen Jr., A. Silveira, S. G. Magalhaes, Ising spin glass in a random network with a Gaussian random field, *Phys. Rev. E* 103 (2) (2021) 022133. doi:10.1103/PhysRevE.103.022133. URL <https://link.aps.org/doi/10.1103/PhysRevE.103.022133>
- [29] C. Kwon, D. J. Thouless, Spin glass with two replicas on a bethe lattice, *Phys. Rev. B* 43 (1991) 8379–8390. doi:10.1103/PhysRevB.43.8379. URL <https://link.aps.org/doi/10.1103/PhysRevB.43.8379>
- [30] J. R. L. de Almeida, D. J. Thouless, *J. Phys. A: Math. Gen.* 11 (1978) 983.
- [31] A. P. Ramirez, Strongly geometrically frustrated magnets, *Annual Review of Materials Science* 24 (1) (1994) 453–480. doi:10.1146/annurev.ms.24.080194.002321. URL <https://doi.org/10.1146/annurev.ms.24.080194.002321>

- [32] A. P. Ramirez, Geometrical frustration in magnetism, Czechoslovak Journal of Physics Supplement 46 (6) (1996) 3247–3254. doi:10.1007/BF02548137.
- [33] E. Sampathkumaran, K. K. Iyer, S. Rayaprol, K. Maiti, Exotic nd 4f electron magnetism in nd 2 rhsi 3, Journal of Magnetism and Magnetic Materials 606 (2024) 172364. doi:10.1016/j.jmmm.2024.172364.
- [34] M. Saccone, F. Caravelli, K. Hofhuis, S. Parchenko, Y. A. Birkhölzer, S. Dhuey, A. Kleibert, S. van Dijken, C. Nisoli, A. Farhan, Direct observation of a dynamical glass transition in a nanomagnetic artificial Hopfield network, Nature Physics 18 (Mar 2022). doi:10.1038/s41567-022-01538-7.